Bearing capacity and driving stresses of open-ended steel pipe piles of Oritkari Quay

La capacité portante et les tensions d'enforcement dans les pieux de tuyau de fer avec bouts ouverts dans le Quai d'Outkari

J. HARTIKAINEN, Professor, University of Oulu, Finland
P. HASSINEN, Research Engineer, Technical Research Centre of Finland
H. KOMULAINEN, Research Assistant, University of Oulu, Finland
E. SLUNGA, Assistant Professor, Helsinki University of Technology, Finland

SYNOPSIS

The quay wall of the Oritkari harbour was constructed of 20 m long, 762 mm in diameter, open-ended steel pipe piles, which were driven through clayey silt into a dense sandy silt layer by a 80 kN hydraulic hammer using a drop height of 0.5...0.8 m. Pile Driving Analyzer (PDA) measurements were done in two stages for 5+5 piles. The ultimate bearing capacities determined by CAPWAP analyses at the end of continous pile driving were 2.7...3.2 MN, which are approx. 35% greater than the geostatically calculated bearing capacities without a soil plug. The dynamic point resistances of the piles were found to be very low, and no solid soil plug developed during driving, although an obvious about 0.5 m long compacted zone inside the pile tip was observed by soundings. Driving stresses of three piles were measured using strain gauges, the results being at the most 60% higher than the stresses calculated by the CAPWAP program.

SITE AND CONSTRUCTION OF THE QUAY

The Oritkari harbour is located on the mouth of the Oulu river south of the city of Oulu. The first stage in the construction of the harbour was completed in 1970.

The stage in the construction work concerned here consisted of a quay designed to accomodate both stern and side-loading vessels with an along-shore length of 170 m and a stern loading breadth of 40 m at right angles to the quay line. The quay is adequate for one or two vessels depending on their size, and could be extended along the shore later if required to take one more vessel. The water depth at the quay is 11.5 m and the height of the quay side above mean water level is 2.4 m.

The dense soil deposit at the site lies at a considerable depth, and is overlain by looser material with a poor bearing capacity which can easily be removed by dredging. Since the water depth at the site was no more than 1.5...2 m, construction of the quay on dry land behind a diversion dam was an obvious solution.

A cross-section showing the construction of the quay is given in Fig. 1. The wall consists of a row of steel pipe piles 762 mm in diameter joined by L and T-angles welded to their sides and fixed rigidly to an edging structure of reinforced concrete, which is also supported by a row of concrete piles. The steel piles extend some 3...4 m into the dense silty sand layer, i.e. to a level of -19.0... -20.5 m.

The head of every second steel pile is anchored by means of a 25 m tie rod to a reinforced concrete anchorage wall which functions by means of passive earth pressure against a granular soil fill. The area lying between the anchorage wall and the wall of steel piles has a foundation of wooden piles 16 m in length driven in at an inclination of 6:1 and fitted with pile caps.

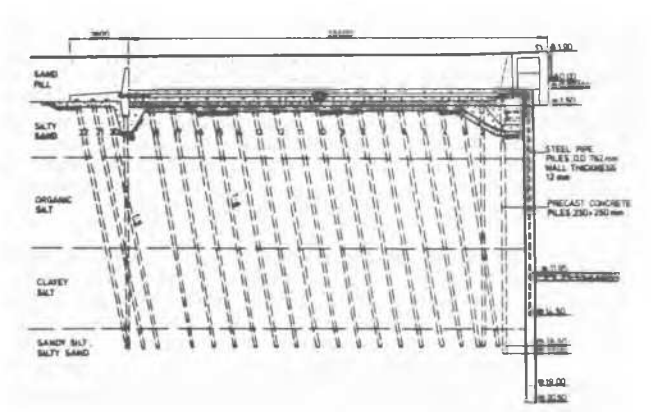

Fig. 1. Cross-section of the quay structure and a soil profile.

The quay structure contains a total of 307 steel pipe piles, 136 concrete piles and 3680 wooden piles. The granular soil fill has a thickness of 3.4 m. Some 266.000 m^3 of soil had to be dredged from the dock basin.

SOIL CONDITIONS

The sea bed was composed of 4...5 m of loose silty sand, beneath which was a 4...6 m layer of highly compressible organic sulphide silt having a water content of 40...60%. Below

these fluvial sediments was 3...6 m layer of hard clayey silt of glacial origin. (Fig. 1) The substrate beneath this consisted largely of dense silty sand.

The weight sounding penetrated to a depth of 16...17 m, thus reaching the dense silty sand layer. The resistance increased markedly at around -14...-18 m. The dynamic probing resistance increased relatively little in the clayey silt layer, but became considerably greater in the silty sand lying below this.

The strength parameters for the soil layers, as used for planning purposes, are shown in Table 1.

Table 1. Dimensioning parameters of soil layer

Soil layer	Effective unit weight γ' (kN/m^3)	Effective friction angle ϕ (^{o})
1. silty sand	8,5	30
2. organic silt	8,0	27
3. clayely silt	9,5	32
4. silty sand	11,0	35

PURPOSE OF THE MEASUREMENTS

The purpose of the stress wave measurements was to obtain information on the behaviour of an open-end steel pipe pile upon driving and ensure that the driving stress would remain within reasonable limits. It was also hoped to compare the ultimate bearing capacities measured at the moment of driving with values calculated from the geostatic stresses. A further topic of interest involved the necessary specifications for the pile driving equipment, and in particular the driving efficiency.

The measurements were performed at two stages in the work, the first being at the beginning of pile driving, with the aim of avoiding damage to the piles while at the same time obviating any unnecessary reductions in the driving force used. The plan was to perform the stress measurements using two complementary methods, a Pile Driving Analyzer (PDA) at the top of the pile and strain gauges placed at various levels along the lower half of the pile.

MEASUREMENT METHODS

The Case method (Goble et al., 1975) involves measurement of the acceleration and the strain of the pile head as functions of time, from which the PDA calculates the particle velocity and plots a force curve. The equipment then uses these velocity and force data to calculate the so called Case bearing capacity, a figure which is recorded separately for each blow of the pile driver in accordance with the adjustments put in by the user. If one wishes to examine the force and velocity curves immediately, an oscilloscope can be linked directly to the PDA. In any case the data are recorded on magnetic tape for later inspection, graphical presentation and further analysis where necessary.

A general outline of the PDA equipment as a whole is presented in Fig. 2, which shows the acceleration and strain transducers attached to the pile, the cables with their junction boxes, the analyzer, based on an MC 68 000 microprocessor, an oscilloscope and a multichannel tape recorder.

INSTRUMENTATION ON THE PILES

Strain gauges were installed at four levels on pile no. 29 and at five levels on nos. 204 and 211, where the numbers are assigned in accordance with the order of driving. The gauges were glued symmetrically on the outer surfaces of opposite sides of the pile, on the positions shown in Fig. 2. The uppermost gauges were located at a level which more or less coincided with the upper boundary of the clayey silt layer towards the end of the pile-driving process, which is also close to the point of maximal bending moment exerted on the pile. This enabled the bending strain to be measured after the dock basin had been dredged. The performing of measurements at different levels also provided an opportunity for assessing the residual stresses remaining in the pile after it had been driven into position.

All the gauges and cables were protected with steel L-angles welded onto the side of the cylinder, and a steel wedge larger in size than the L-angles was welded onto the tip of the pile with a gap of 1 mm between it and the L-angle. This gap avoids the forces exerted on the wedge to be transmitted to the gauges. Although the protective angles themselves transmit some of the force, the error arising in this way is small, as the effect of this force is spread over a broad area of the cylinder at the point where the gauge is located.

The 8...10 cables reaching the top of the pile (20 on pile no. 204) were plugged into connect-

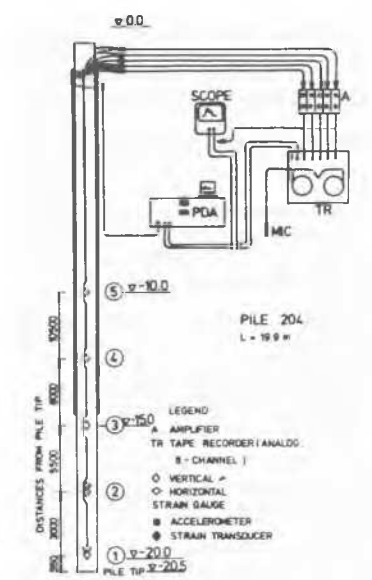

Fig. 2. Scheme of instrumentation.

ing cables, these then leading to the amplifier unit. The five amplifiers available effectively restricted the number of signals to be recorded to five, although a sixth gauge could also be monitored by alternation. The connection scheme is to be seen in Fig. 2. Two of the eight channels on the tape recorder were used to record the PDA force and velocity signals, five for the force curves and one for voice recording.

PILE-DRIVING EQUIPMENT

The driving of steel pipe piles 762 mm in diameter required an unusually large hammer and pile helmet, while the length of the piles, 20 m, and the order in which they were to be driven necessitated a rig of considerable height, which in turn meant ensuring that the base machine was sufficiently heavy to guarantee stability (Fig. 3a).

Fig. 3a) Driving of the pipe pile wall and 3b) the 80 kN hydraulic drop hammer, Junttan.

The hydraulically operated hammer constructed on an excavator chassis by Savonvarvi Oy employed at Oritkari proved highly suitable for this purpose (Fig. 3b), the two parallel lifting hydraulic cylinders being capable of maintaining a frequency of 60...70 blows per minute with a 80 kN hammer at a drop height of 0.5 m. The maximum drop height attainable was 0.8 m. The height of the rig was 38 m and the total weight of the equipment something over 1000 kN.

The pile helmet consisted of 100 mm thick steel plate, a centering cone, an elastic part made of azobe wood and a steel frame surrounding this. The elastic part was 370 mm high and square in cross-section (450x450 mm). The grain of the azobe wood ran in a vertical direction.

INITIAL STRESS WAVE

The driving of steel piles does not always require the use of a pile helmet, since steel is a sufficiently tough material to withstand short peak stresses, even ones in excess of the static yield point. Without the helmet, the stress wave is of short duration and rapidly rising in form, which is undesirable as far as the penetration velocity of the pile is concerned. The form of the stress wave can be adapted by a pile helmet with suitable properties or by an elastic hammer construction.

When a blow is applied to an elastic pile using a rigid hammer without a pile helmet the resulting initial stress wave obeys the equation, (Bredenberg, 1982)

$$F_i(t) = Z \cdot v \cdot e^{-\frac{Z}{m}t} \qquad (1)$$

where, F_i = impact force
Z = $\frac{AE}{c}$ pile impedance,
A = cross-sectional area of pile
E = elastic modulus of pile
v = particle velocity of the head of the pile, = hammer velocity in this case,
m = mass of the hammer,
t = time.

In practice the wave front is not vertical but shows a brief rising phase. Similarly the wave never reaches its theoretical peak.

The piles studied here were driven using a pile helmet with a static spring constant of 8592 MN/m, corresponding to 54% of the rigidity of an equal length of pile (370 mm), i.e. the pile helmet was fairly rigid. The mass of the hammer was 8000 kg and its legth 3.0 m.

The initial stress wave (Fig. 4) was measured early in the pile driving process, when the tip was still only at a depth of 3.5 m. The first reflected wave was the tension wave from the tip, so that the initial stress wave

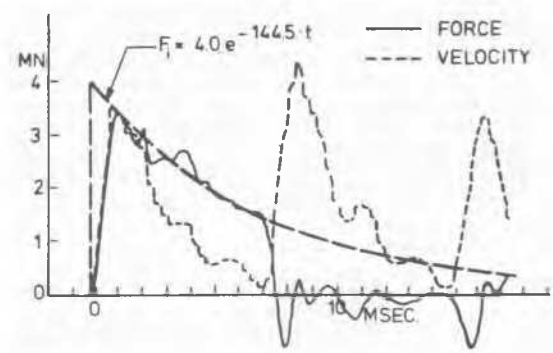

Fig. 4. Force and velocity of the head of pile 204 as functions of time at the beginning of driving.

alone could be examined during a time of $\frac{2L}{c}$. The wave diminished exponentially in the manner given by equation.

$$F_i(t) = Z \cdot v \cdot e^{-144.5t} \qquad (2)$$

Its rise time is 0.6 ms and the strain velocity brought about by the wave front $\dot{\varepsilon} = 0.88 \frac{1}{s}$.

The acceleration of the pile head is obtained from the equation

$$\ddot{x} = \dot{\varepsilon} \cdot c \qquad (3)$$

in which c = wave velocity = 5139 m/s. This gives an acceleration of 4500 m/s^2, or 460 g.

Since the pile helmet was highly rigid, it caused rather little alteration in the form of this wave, protracting the time slightly, but scarcely reducing its maximum amplitude. The maximum measured stresses varied in the range 105...163 N/mm^2 with drop heights of 0.5...0.75 m (Table 2).

Table 2. Calculated and measured maximum driving stresses (MPa)

Pile no.	drop height (m)	max.imp.stress calc.	max. measured stresses meas.at pile head	at diff.levels
25	0,5	121	83	121
27	"	"	118	140
29	"	"	80	105 -
29	0,8	156	114	138 95 ②
204	0,5	121	137	137 146 ③
"	0,75	151	163	163 160 ③
211	0,7	145	140	140 148 ③ ④

About 60...75% of the kinetic energy of the hammer was transmitted to the pile, this proportion being unaffected by the above variations in drop height. Figures of around 90% have been obtained for the efficiency of a rigid hammer without pile helmet in laboratory experiments (Bredenberg 1982).

REFLECTION OF STRESS WAVES

No strong reflected compression waves are created provided that the dynamic skin resistance of the pile is relatively evenly distributed and the point resistance is small, in which case the sum of the gradually weakening initial wave and the reflected waves does not exceed the strains imposed by the initial wave. If one pictures the skin friction of the pile as being concentrated in a set of points, the amplitude F_i of the incoming wave decreases at each point by (Fischer, 1984):

$$F_{i,j+1} = F_{i,j} - \frac{R}{2}j, \qquad (4)$$

in which $F_{i,j}$ = amplitude of wave which has passed point j,
R_j = skin resistance at point j.

The compression wave $F_R = \frac{R}{2}j$ is reflected upwards at point j, whereas if $R > 2 F_i$, the whole wave will be reflected in the form of a compression wave, summing with the incoming waves. If the skin frictions caused by the upward and downward-moving stress waves are equal, a residual compressive force $\frac{R}{2}$ remains between two consecutive friction points in the pile. The following stress wave will then tend to be reflected as a compression wave under the influence of this residual force. The soil model is assumed here to be a rigid-plastic one.

A number of computer programs have been devised for analysing reflected waves recorded at the head of a pile. The CAPWAP program (Goble et al., 1975), which employs one-dimensional wave equation, enables one to calculate the distribution of the dynamic skin friction along the length of the pile and the stresses at any given point on the pile. The program uses parameters supplied by the user together with the resistance distribution to plot a curve for the force developing at the head of the pile, which is fitted as closely as possible to the measured power curve.

CAPWAP analyses were performed on the last blows applied to 6 piles. The skin resistance distributions for piles nos. 25, 29 and 33 are presented in Fig. 5a and for piles nos. 204 and 211, situated about 150 m away, in Fig. 5b. The friction in piles 25 and 29 is seen to be concentrated in an area about 4...7 m from the tip, the strongest skin friction of pile 33 being noted 1...5 m from the tip. The point resistances of all the piles are very small, and a half of the total skin resistance is shown to be concentrated in an area 3...6 m from the tip.

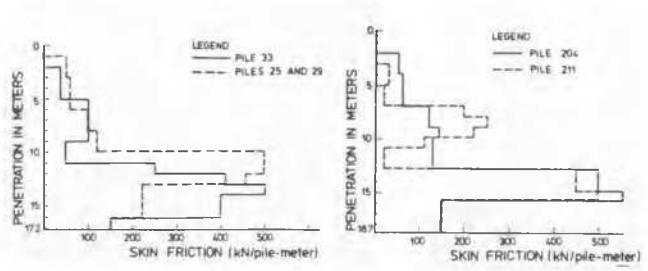

Fig. 5. Skin friction during driving calculated by CAPWAP a) piles 25, 29 and 33 b) piles 204 and 211.

Force and velocity curves for pile no. 25 are presented in Fig. 6a, in which the force wave includes a strong reflected compression wave with its peak 5.2 ms after that of the initial wave. The location of the skin friction concentration is given by the equation

$$x = \frac{c \cdot t_{max}}{2}, \qquad (5)$$

in which x = distance of skin friction concentration from measurement point,
t_{max} = time differential between peaks in the initial and reflected waves.

The calculated skin friction in pile 25 is greatest 13.4 m below the measurement point, i.e. 3.8 m from the tip of the pile, a result which is at variance with the situation in Fig. 5a, which shows the skin friction to be concentrated approx. 2 m upper.

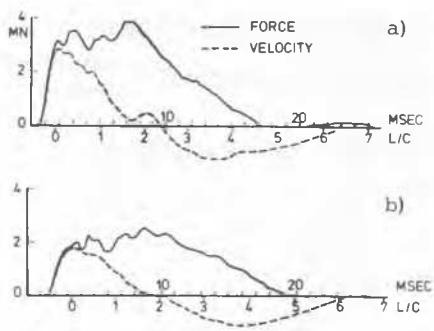

Fig. 6. Force-time and velocity-time curves of the head of a) pile 25 at final penetration b) pile 29 1,0 m above final penetration.

The driving stresses recorded by the gauges on pile 29 reached their maximum after a pause of 1½ days. This stress was only 10% greater than the impact stress. This is illustrated in Fig. 6b, which depicts the first blow after the interval. In this case the CAPWAP analysis places the concentration of friction somewhat higher.

The force curve recorded on the top of pile no. 204 shows a local minimum value some time after the peak in the initial wave (Fig. 7a). The wave reflected from the tip must thus be a tension wave with a simultaneous increase in velocity. The amplitudes of the compression waves reflected from the skin surface of the pile are relatively small during the $0...\frac{2L}{c}$. The exponentially decreasing initial stress wave is represented by a dotted line.

Stress waves recorded at the top of pile no. 204 and at the levels 1...4 are depicted in sections b...e of Fig. 7, on which the corresponding force curves obtained from the CAPWAP analysis are indicated with dotted lines. The measured and theoretical curves correspond relatively well at level 4, but at levels 2 and 3 the measured wave amplitudes are 60% greater than the calculated ones. The overall lengths of the waves more or less correspond. The tension wave from the tip is slightly earlier noticed at levels 2, 3 and 4 than is given by CAPWAP, while the incoming compression and tension waves at level 1 are practically simultaneous, the time discrepancy, approx. 0.2 ms, being shorter than the rise time of the compression wave, so that the amplitude remains small. The strength of the tension wave is roughly 70...80% of that of the compression wave.

The differences between the calculated and measured stresses may be caused by residual stresses, which were highest near the tip of pile 204. The max. residual stress was approx. 100 N/mm^2 in tension, measured 5 hours after pile driving had been finished. The highest compressive residual stress was 140 N/mm^2 in pile 29.

BEARING CAPACITY

The bearing capacity of a pile as determined by the Case method may be regarded as being most reliable in noncohesive soils. Thus the

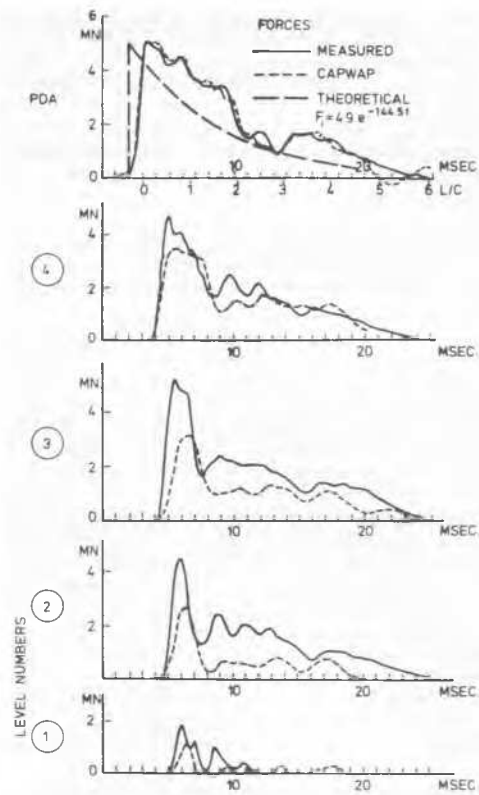

Fig. 7. Measured and calculated force-time curves at different levels of pile 204 at the last blow.

ultimate bearing capacities calculated by the method in silty soils are those which deviate most markedly from the actual values, due to the great variation and poor predictability of the damping constant J_C in such soils. The damping constant can be evaluated more precisely using the CAPWAP program.

The ultimate bearing capacity was determined by means of CAPWAP analysis for 6 piles, the results varying in the range 2.7...3.2 MN, corresponding to Case damping constants of 0.40...0.55. By this stage the tip of the pile was in the silty sand layer, for which a damping constant of 0.15 is recommended. The value for the clayey silt is much higher, 0.55 on average. The quake parameter was 0.17 ...0.23 cm for pile no. 204 and otherwise consistently 0.20 cm.

It is difficult to calculate the point resistance of an open-ended pipe pile. The figure is obviously low provided that a soil plug does not form at the tip, but the probability of this phenomenon depends on the soil type, the coarse of the inner surface of the cylinder and the diameter of the cylinder at least. In a dense sand layer a plug can develop even during the driving of the pile. Also, plugging due to static loading and plugging due to dynamic loading are two quite different things.

Since the piles studied here are relatively short, the point resistance has a considerable effect on bearing capacity, the geostatically

calculated ultimate bearing capacities varying according to the method used (Table 3), ("Veiledning ved pelefundamentering", 1973; Meyerhof, 1976; Poulos, Davis, 1980) and the degree of plugging within the range 1.8... 3.4 MN. The external and internal skin resistances are assumed in the calculations to be equal. The observed permanent sets at last blows varied between 4...8 mm.

Table 3. Bearing capacity (MN) of pipe piles according to three calculation methods, Case and CAPWAP. (Lower limit without and upper with plug.)

	Pile No.			
CALC. METHOD	25	29	204	211
Meyerhof (1976)	2.0...3.1	2.0...3.1	2.3...3.3	2.3...3.3
Poulos (1980)	3.3	3.3	3.4	3.4
Veiledning..(1973)	2.1...2.8	2.1...2.8	2.2...2.6	1.8...2.3
Case, J_C = 0.45	3.4	4.3	3.0	2.7
CAPWAP	3.0	3.0	3.0	2.8

The dynamically determined ultimate bearing capacities lie in the upper half of the range of variation of the statically calculated values, a pattern which would seem to gain support from the mild plugging effect observed in the dynamic probing tests (Fig. 8), although the CAPWAP analysis does show any evidence of plugging near the tip of the pile.

CONCLUSIONS

The bearing capacities of the piles, as determined by CAPWAP analysis, were in the range 2.7...3.2 MN, corresponding to damping constants of J_C = 0.40...0.55 in the Case method. All the piles had a point resistance of less than 0.2 MN.

The above values were about 35 % greater than the ultimate bearing capacities, calculated geostatically and including only the skin resistance. It can be expected that the bearing capacity would still increase considerably after the dissipation of excess pore water pressure. The skin friction, as calculated using the CAPWAP program, was with one exception concentrated in the clayey silt horizon 3...7 m from the tip of the pile, whereas the dynamic probing resistance was greatest close to the tip. This suggests, that the dynamic and static skin resistances are located at different depths.

The soundings showed considerable compaction of the soil inside the pipe pile about 0.5 m from the tip. This could be interpreted partly as representing a soil plug, but at least it did not increase the point resistance. The data on the progress of the first blows after a pause tended slightly to point to the possible formation of a static soil plug upon the dissipation of the excess pore water pressure.

The initial stress wave followed the theoretical wave form relatively closely, the calculated stresses proving quite valid. The stresses existing in the bottom half of the pile were found to be much greater than those calculated by the CAPWAP program, however, exceeding them by as much as 50...60%. When only PDA measurements are used to monitor stresses

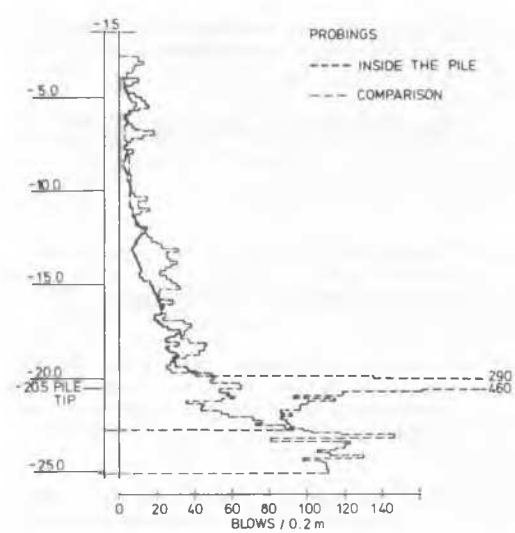

Fig. 8. Dynamic probing through pile 206 in comparison with a probing 5 m away.

in the pile a 60% increase is too large when operating close to the yield point of steel. The highest stresses observed in this research were nevertheless very much smaller than the maximum permitted values.

Construction of the steel pipe pile wall was highly successful, and the pile driving operation was carried through efficiently without increasing the risk of damaging the piles.

ACKNOWLEDGEMENTS

This research was sponsored by Rautaruukki Ltd (The finnish state owned steel company) and it was supported by the client, City of Oulu and by the contractors, YIT Ltd and OMP Ltd. Structural design of the quay was made by Voimarakenne Ltd and geotechnical design by PSV Ltd.

REFERENCES

Goble, G.G., Garland Likins Jr., Rausche, F. (1975). Bearing capacity of piles from dynamic measurements. Final report, Dept. of Civil Engineering, Case Western Reserve University, Ohio.

Fischer, H.C. (1984). Stress wave theory for pile driving applications, lecture. Second Int. Conf. on the Application of Stresswave Theory on Piles, Stockholm, pp. 43-46.

Bredenberg, H. (1982). Dynamic test loading of point bearing piles. Doctor thesis, Royal Institute of Technology, Dept. of Soil and Rock Mech., Stockholm, pp. 56-80,250-262.

"Veiledning ved pelefundamentering". Rules for Pile Foundation (1973). The Norwegian Pile Committee. Oslo, pp. 25-33.

Meyerhof, G.G. (1976). Bearing capacity and settlement of pile foundations. ASCE J. Geotech. Div. vol 102, GT3, pp. 199-217.

Poulos, H.G., Davis, E.H. (1980). Pile foundation analysis and design. J. Wiley & Sons, New York, pp. 18-30.